Journal of Sol-Gel Science and Technology (2019) 92:293–303
https://doi.org/10.1007/s10971-019-05039-7

ORIGINAL PAPER: NANO- AND MACROPOROUS MATERIALS (AEROGELS, XEROGELS, CRYOGELS, ETC.)

Check for updates

Formation of mesoporous structure in Al_2O_3–$NaAlO_2$-based materials produced by template synthesis

Inna A. Yamanovskaya[1] · Tatyana V. Kusova[1] · Anton S. Kraev[1] · Alexander V. Agafonov[1] · Gulaim A. Seisenbaeva[2] · Vadim G. Kessler[2]

Received: 28 December 2018 / Accepted: 28 May 2019 / Published online: 10 June 2019

Abstract

Mesoporous alumina and γ-Al_2O_3–$NaAlO_2$ composites with different morphology were produced by soft chemistry methods using polyethylenimine (PEI), pluronic P123 (P123), and polymer–colloid complex (PCC) derived from them as templates in solution. Sodium aluminate was applied as an additive for production of the mesoporous γ-Al_2O_3–$NaAlO_2$ composite. The obtained samples were characterized by scanning and transmission electron microscopy, atomic force microscopy, Fourier transform IR spectrometry, X-ray diffraction analysis, and low-temperature N_2 adsorption–desorption analysis. The effect of sodium aluminate introduction on the morphological features of the obtained samples was investigated. Mesostructured aluminum oxide obtained using individual templates such as P123 and PEI possesses cylindrical pores, whereas applying PCC resulted in the formation slit-shaped pores. The produced mesoporous aluminum oxide and γ-Al_2O_3–$NaAlO_2$ composite had a narrow pore size distribution and large surface area. This approach was demonstrated to allow for the control of pore sizes and shapes.

Graphical Abstract

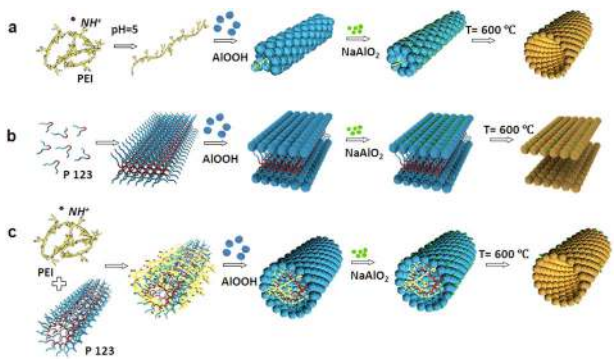

Supplementary information The online version of this article (https://doi.org/10.1007/s10971-019-05039-7) contains supplementary material, which is available to authorized users.

✉ Vadim G. Kessler
vadim.kessler@slu.se

[1] Krestov Institute of Solution Chemistry of the Russian Academy of Sciences, Akademicheskaya St., 1, 153045 Ivanovo, Russia

[2] Department of Molecular Sciences, Swedish University of Agricultural Sciences, Box 7015, 750 07 Uppsala, Sweden

Highlights

- Mesoporous alumina and γ-Al_2O_3–$NaAlO_2$ composites with different morphology were produced by soft chemistry approach in solution.
- Polyethylenimine (PEI), pluronic P123 (P123), and polymer–colloid complex (PCC) derived from them were used as templates.
- Obtained porous materials were characterized by SEM, AFM, FTIR, XRD, and gas sorption techniques.
- Formation mechanisms for mesoporous structures were elucidated and compared for synthesis of pure alumina and of γ-Al_2O_3–$NaAlO_2$ composites.

Keywords Aluminum oxide · Sol–gel method · Polymer–colloid complex · Supramolecular self-assembly · Ordered nanoporous structure

1 Introduction

Mesoporous aluminum oxide is of interest as an adsorbent, a catalyst and an active phase carrier substrate owing to its attractive acid–base and textural properties [1–8]. Most-promising methods in obtaining mesoporous aluminum oxide structures are based on chemical transformations in solutions [9, 10]. A promising and still relevant direction is developing approaches to control the formation of mesoporous structures of materials exploiting liquid phase synthesis. An important role in producing mesoporous aluminum oxide structures is played by the template applied for mesophase formation [11–16]. Previously, we have demonstrated the prospects of using polyethyleneimine for preparation of the mesoporous catalysts based on alumina–sodium aluminate composite materials with pore diameter of 7–11 nm and highly developed surface for esterification of vegetable oils [5]. Moreover, methods based on application of the mesostructured polymer–colloid complexes (PCCs) using different templates to affect both the size of the pores and also their shapes have been described by us recently [6, 7]. Thus, the main aim of the present work was to investigate the influence of sodium aluminate ($NaAlO_2$) used as an additive on the formation of the internal mesoporous structure of aluminum oxide (γ-Al_2O_3) obtained with the application of Pluronic P123, polyethylenimine (PEI) and PCC based on them. The selected surfactants were used as the templates for the formation of mesophases, on which the precursors of aluminum oxide were adsorbed.

2 Experimental

2.1 Material

Aluminum isopropoxide $Al(OC_3H_7)_3$, nitric acid (HNO_3, 68.4 wt%), polyethylenimine ($H(–NHCH_2CH_2)nNH_2$, $M_w = 25{,}000$), Pluronic P123 ($(C_3H_6O.C_2H_4O)_x$, $M_n = 5800$), sodium aluminate ($NaAlO_2$) were purchased from Sigma-Aldrich and used without further purification.

2.2 Synthesis of mesoporous γ-aluminum oxide

Synthesis of the nanostructured polymer-colloidal complexes using different templates in aqueous medium under constant mixing was carried out using slightly modified approaches recently reported by our group [6, 7]. The synthesis scheme of γ-Al_2O_3 is presented in Fig. 1a.

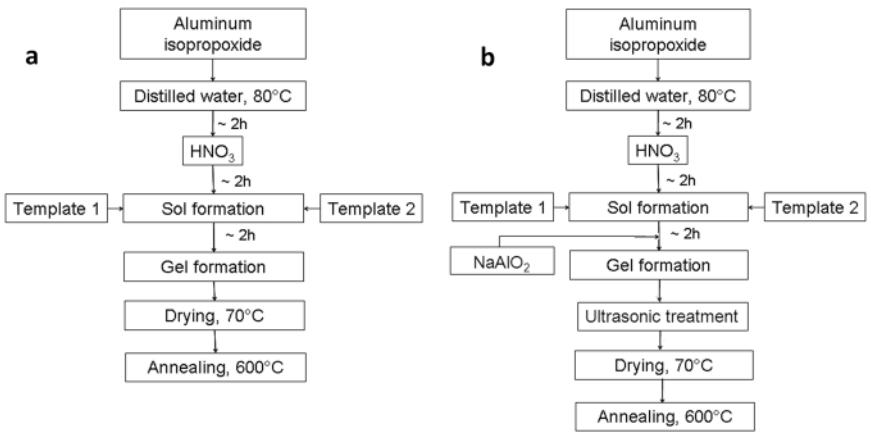

Fig. 1 Scheme of synthesis for nanostructured aluminum oxide **a** and for templated of γ-Al_2O_3–$NaAlO_2$ samples

In brief, 100 ml of distilled water was initially heated to 80 °C. Then, 16 g of aluminum isopropoxide was added in small portions to the reaction medium. The mixture was homogenized for 2 h. The peptization process was used to form the sol. For this, 1.5 ml of concentrated nitric acid was added to the flask. Then, a polyelectrolyte or/and surfactant was added to the boehmite sol in the required amount. The obtained aluminum hydroxide sol was dried at 70 °C. Finally, the obtained powder was calcinated at 600 °C for 4 h to form an active alumina.

2.3 Synthesis of mesoporous γ-Al_2O_3–$NaAlO_2$ composite

The mesoporous γ-Al_2O_3–$NaAlO_2$ composite was synthesized in aqueous medium under constant mixing according to the following scheme (Fig. 1b). For this, 16 g of $Al(C_3H_7O)_3$ was added in small portions to 100 ml of distilled water initially heated to 80 °C. The mixture was homogenized for 2 h. The obtained white precipitate of aluminum hydroxide was peptized by 1.5 ml of concentrated nitric acid. Then, either Pluronic P123, or Pluronic P123 together with PEI to be used as the templates were added to the boehmite sol in the required amount for the formation of the PCCs in the following ratio: Al_2O_3: P123 = 2:1 and Al_2O_3: PEI: P123 = 2:1:1. Introduction of the selected templates was used to form a porous structure uniformly distributed throughout the volume. After prolonged stirring, an active phase, sodium aluminate, was added to the flask. The $NaAlO_2$ content was 60% of the total catalyst weight. The obtained gel was first ultrasonicated for better homogenization of the mixture and then dried at a temperature of 70 °C. The obtained powder was calcined at 600 °C for 4 h to form a mesoporous γ-Al_2O_3–$NaAlO_2$ composite by removing the organic template. Mass concentrations of the reagents for preparing each of the mesostructured samples are summarized in Table 1.

2.4 Characterization

"DRON-2" X-ray diffractometer with a copper anode was used for X-ray powder diffraction measurements. The infrared (IR)-spectra of the synthesized materials were obtained using Fourier transform IR-spectrometer Avatar 360 FTIR ESP. The adsorption/desorption isotherm studies were carried out with Nova Quantachrome 1200 instrument. The values of specific surface areas were calculated using Brunauer–Emmett–Teller (BET) model [17] and pore size distribution was obtained applying Barrett–Joyner–Halenda (BJH) approach [18]. Scanning electron microscopy (SEM) studies were carried out with Hitachi TM-1000-μ-DeX and VEGA3 TESCAN instrument (Brno, Czech Republic). Atomic force microscopy investigations were carried out with Bruker FastScan with ScanAsyst instrument, using FastScan B cantilevers in air in the ScanAsyst mode. TEM investigation was carried out with JEOL JEM-1011 transmission electron microscope with digital camera ORIUS SC1000W. Acceleration voltage 80 kV.

3 Results and discussion

3.1 X-ray diffraction analysis

The results of the X-ray diffraction analysis for the annealed and non-annealed γ-Al_2O_3 samples prepared in aqueous medium by using PEI (3a), P123 (3b), PCC (3c) as templates are presented in Fig. 2a–c.

According to the X-ray diffraction study, the non-annealed γ-Al_2O_3/template samples mainly consisted of partially crystallized boehmite. In particular, γ-Al_2O_3/PEI has well-defined peaks at 2θ = 21°, 37°, 46°, 58°, 68° (Fig. 3a); γ-Al_2O_3/P123 has well-defined peaks at 2θ = 14.5°, 28.5°, 38.8°, 49.2°, 64.8° (Fig. 3b); γ-Al_2O_3/PCC has well-defined peaks at 2θ = 13.5°, 18.0°, 23.1°, 28.0°, 38.2°, 49.0°, 64.8° (Fig. 3c). After γ-Al_2O_3/template samples annealing at 600 °C, the peaks that appear on the diagrams indicate the presence of the γ-Al_2O_3 crystalline phase in the samples. The annealed γ-Al_2O_3/PEI, γ-Al_2O_3/P123, γ-Al_2O_3/PCC have the peaks at 2θ = 15°, 22°, 29°, 40°, 51°, 66°, 72° (Fig. 3a); 2θ = 38.0°, 45.5°, 66.2° (Fig. 3b); and 2θ = 21.0°, 38.0°, 46.0°, 66.5° (Fig. 3c), respectively. This meant that the annealing of the initial γ-Al_2O_3/template samples resulted in template removal and formation of a highly-ordered mesoporous γ-Al_2O_3 structure.

Table 1 Reagent concentrations in solution for synthesis of the γ-Al_2O_3/template and γ-Al_2O_3–$NaAlO_2$/template samples

Sample name	Reagent content, wt. %					
	H_2O	$Al(C_3H_7O)_3$	$NaAlO_2$	$HNO_{3\ conc}$	PEI	P123
γ-Al_2O_3/PEI	82.82	13.25	–	0.62	3.31	–
γ-Al_2O_3/P123	82.82	13.25	–	0.62	–	3.31
γ-Al_2O_3/ PCC	82.82	13.25	–	0.62	1.66	1.66
γ-Al_2O_3–$NaAlO_2$/PEI	82.03	13.13	1.97	1.23	1.64	–
γ-Al_2O_3–$NaAlO_2$/P123	82.03	13.13	1.97	1.23	–	1.64
γ-Al_2O_3–$NaAlO_2$/PCC	82.03	13.13	1.97	0.62	0.82	0.82

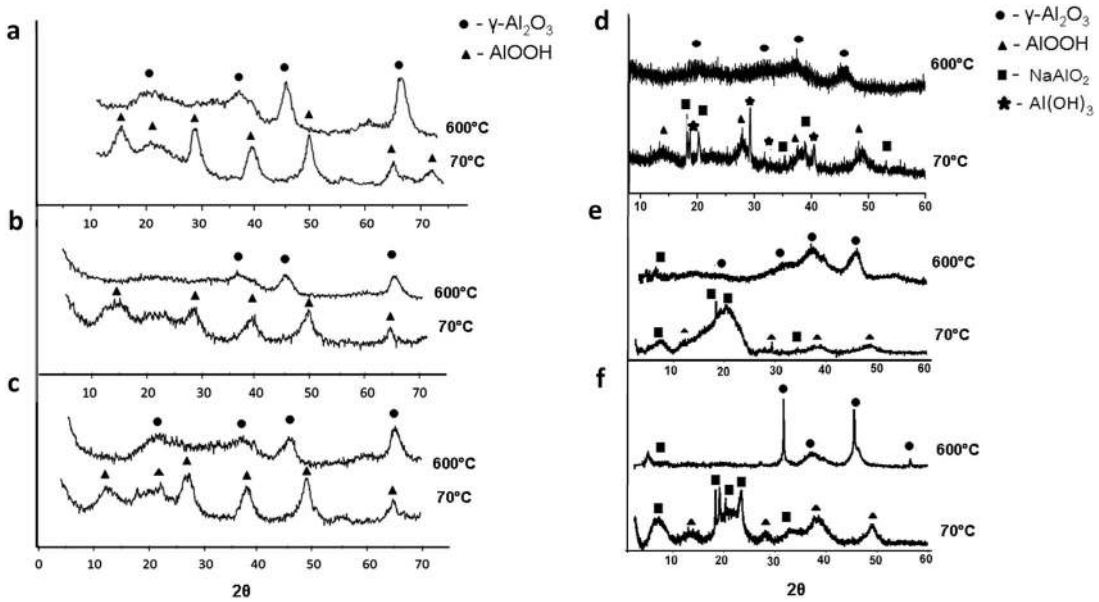

Fig. 2 X-ray diffractograms of the γ-Al_2O_3 **a–c** and γ-Al_2O_3–$NaAlO_2$ **d–f** samples obtained with different templates: PEI **a**, **d**; P123 **b**, **e**; PCC **c**, **f**

XRD patterns for the annealed and non-annealed γ-Al_2O_3–$NaAlO_2$ samples, prepared in aqueous medium by using PEI (2d), P123 (2e), PCC (2 f) as the templates are displayed in Fig. 2d–f. As the non-annealed γ-Al_2O_3/template samples, the non-annealed γ-Al_2O_3–$NaAlO_2$/template samples obtained by using different templates also consist of partially crystallized boehmite. In particular, γ-Al_2O_3–$NaAlO_2$/PEI shows the peaks at 2θ values of 13.6°, 23.5°, 33.9°, 35.8°, 49.1° (Fig. 2d); γ-Al_2O_3–$NaAlO_2$/P123 shows the peaks at 2θ values of 2θ = 27.2°, 38.1°, 48.5° (Fig. 2e); γ-Al_2O_3– $NaAlO_2$/ PCC 2θ = 12.6°, 27.6°, 38.4°, 48.4° (Fig. 2f).

The samples have well-defined peaks in the following regions: for γ-Al_2O_3–$NaAlO_2$/PEI 2θ = 13.6°, 23.5°, 33.9°, 35.8°, 49.1° (Fig. 2d), γ-Al_2O_3–$NaAlO_2$/P123 2θ = 27.2°, 38.1°, 48.5° (Fig. 2e), γ-Al_2O_3–$NaAlO_2$/PCC 2θ = 12.6°, 27.6°, 38.4°, 48.4° (Fig. 2f), as well as the peaks at 2θ = 18.2°, 20.2°, 29.1°, 31.8°, 35.3° (γ-Al_2O_3–$NaAlO_2$/PEI (Fig. 2d)), 2θ = 7.3°, 18.6°, 29.0°, 34.7° (γ-Al_2O_3–$NaAlO_2$/P123 (Fig. 2e)), 2θ = 6.5°, 18.4°, 19.5°, 20.3°, 23.5°, 31.7° (γ-Al_2O_3–$NaAlO_2$/PCC (Fig. 2f)), corresponding to the crystalline phase of $NaAlO_2$. There were also peaks corresponding to the crystalline phase of $Al(OH)_3$: 2θ = 18.7°, 38.9°, 40.5° (γ-Al_2O_3–$NaAlO_2$/PEI (Fig. 2d)).The peaks that appear on the diagrams after sample annealing at 600 °C indicate the presence of the γ-Al_2O_3 crystalline phase in the samples. The γ-Al_2O_3–$NaAlO_2$/PEI, γ-Al_2O_3–$NaAlO_2$/P123 and γ-Al_2O_3–$NaAlO_2$/PCC samples have reflections in the following regions: 2θ = 19.8°, 31.8°, 36.9°, 45.9° (Fig. 2d); 2θ = 31.6°, 37.5°, 45.5° (Fig. 2e), 2θ = 19.7°, 31.7°, 37.3°, 45.4° (Fig. 2f), respectively. There were also peaks corresponding to the crystalline phase of $NaAlO_2$:
2θ = 6.7°, 9.9° (γ-Al_2O_3–$NaAlO_2$/P123 (Fig. 2e)), 2θ = 8.6° (γ-Al_2O_3–$NaAlO_2$/PCC (Fig. 2f)). Thus, the obtained results showed that during the calcination of the samples at 600 °C, the template is removed, forming a mesoporous structure of γ-Al_2O_3–$NaAlO_2$ composite. The introduction of sodium aluminate into the synthesis of γ-Al_2O_3 has an effect on the crystal structure of the samples. As it shown in our previous work [5], during the thermal treatment of the samples, there occurs a partial dissolution of the sodium aluminate phase as well as the transition from the boehmite phase to γ-Al_2O_3.

3.2 Fourier transform IR-spectroscopy

All spectra of the materials (See Supplementary figures S1 and S2 for non-annealed and annealed at 600 °C γ-Al_2O_3 and γ-Al_2O_3–$NaAlO_2$ composite respectively, synthesized using PEI (a), P123 (b), and PCC (c) as marked in both images) have characteristic absorption bands of Al–O and Al–O–Al fragments around 565 cm^{-1}, 593 cm^{-1}, 629 cm^{-1}, 794 cm^{-1}, 805 cm^{-1}. The wavenumber region ~ 3444–3446 cm^{-1} as well as the region ~ 1640–1382 cm^{-1} is associated with molecular vibrations of H_2O, adsorbed on the surface. The system also displays bands corresponding to the stretching vibrations of hydroxyl OH groups and vibrations of hydrogen bonds of the O – H…O type in the region of 3746–3044 cm^{-1}. The spectra of the non-annealed samples in the wavenumber regions of 2959–2913 cm^{-1} and 1259–1401 cm^{-1} contain spectral bands of CH_3, CH_2, and CH [19] groups of alkyl chains, which

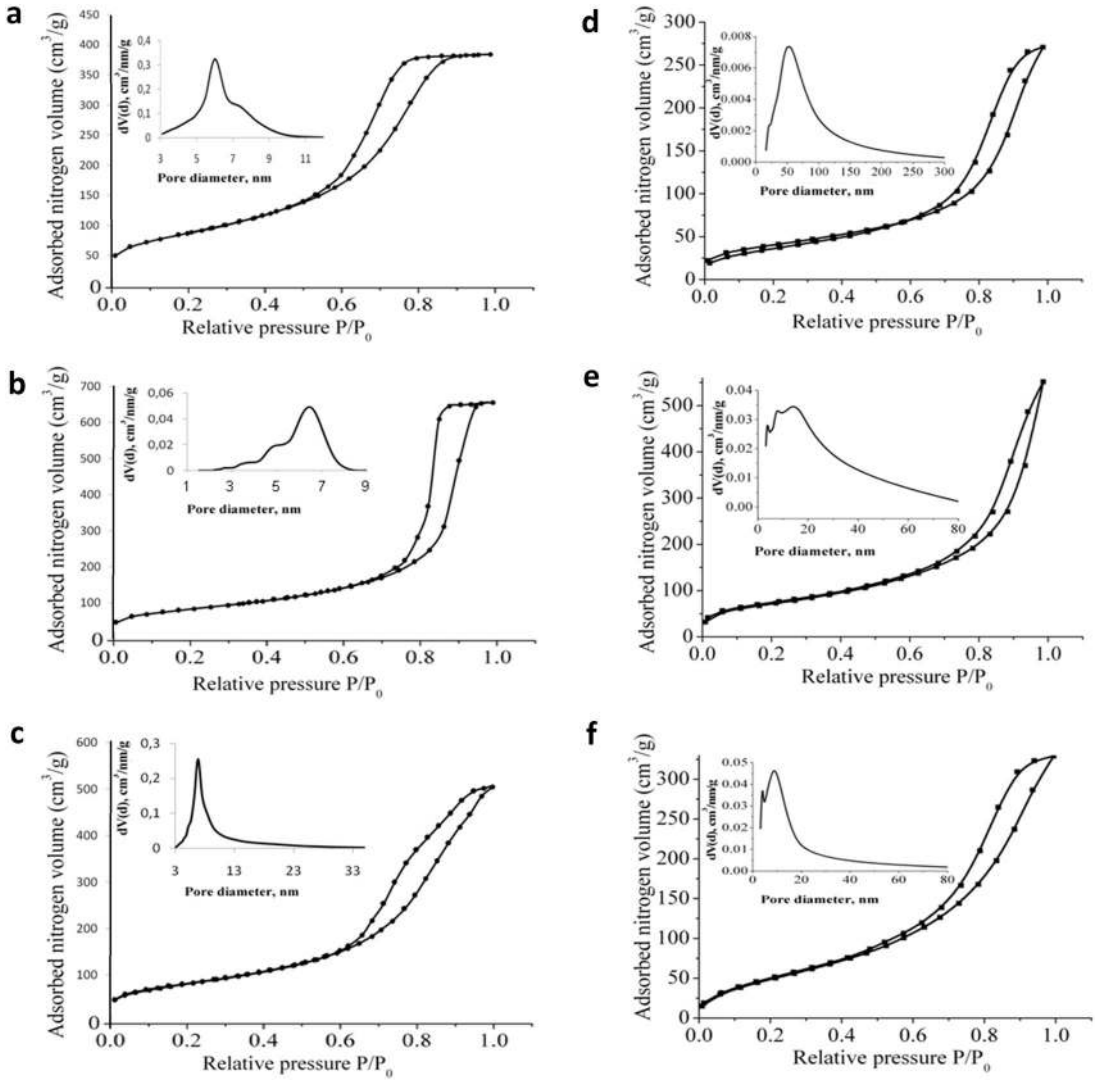

Fig. 3 Results of low-temperature nitrogen adsorption/desorption of the γ-Al_2O_3 **a**–**c** and γ-Al_2O_3–$NaAlO_2$ **d**–**f** samples obtained with different templates: PEI **a**, **d**; P123 **b**, **e**; PCC **c**, **f**

indicates that the composite includes the organic phase. After annealing, the bonds characteristic of the organic component in the materials were removed practically completely.

3.3 Low-temperature nitrogen adsorption–desorption

The low-temperature nitrogen adsorption–desorption results of the γ-Al_2O_3 and γ-Al_2O_3–$NaAlO_2$ samples prepared using PEI, P123, PCC as the templates, are presented in Fig. 3a–c and Fig. 3d–f, respectively. The textural characteristics of the obtained samples are shown in Table 2.

The authors of [10, 16] have shown that using PEI as the template results in the formation of ordered mesopores of the same diameter. Indeed, the hysteresis loop profile of γ-Al_2O_3/PEI (Fig. 3a) is typical of the cylindrical pores of the type H1 [17]. The pore size distribution of γ-Al_2O_3/PEI (Fig. 3a) is wider than in the previous samples (γ-Al_2O_3) but is much narrower than that of the industrial analogs. Pores are formed by organic phase burnout under annealing and have the same size and shape as the supramolecular polyethyleneimine features. The γ-Al_2O_3/P123 sample obtained by using P123 as the template has a hysteresis loop in the mesopore region (Fig. 3b). In the case of this sample, the hysteresis loop shape coincides with the classical one (type H1) and corresponds to the presence of cylindrical pores [17]. The pore size distribution in the sample (γ-Al_2O_3/P123) lies in the region of 3–9 nm (Table 2), which is typical of ordered mesoporous materials. The hysteresis loop of the γ-Al_2O_3/PCC sample obtained by using the polymer–colloid complex (PCC) also lies in the mesopore region (Fig. 3c). The hysteresis loop profile of γ-Al_2O_3/PCC

Table 2 Textural characteristics of synthesized samples

Sample name	Modifying agent	Pore type	S_{BET}, m^2/g	S_{mesop}, m^2/g	D_p, nm	V_p, cm^3/g
γ-Al_2O_3	–	Ink-bottle-shaped	177	202	4.7	0.211
γ-Al_2O_3/PEI	PEI	Cylindrical	317	405	7.5	0.594
γ-Al_2O_3/P123	P123	Cylindrical	295	363	6.9	1.013
γ-Al_2O_3/PCC	PCC	Slit-shaped	297	85	10.5	0.781
γ-Al_2O_3–$NaAlO_2$	–	Ink-bottle-shaped	68	134	4.1	0.140
γ-Al_2O_3–$NaAlO_2$/PEI	PEI	Cylindrical	119	144	11.6	0.330
γ-Al_2O_3–$NaAlO_2$/P123	P123	Slit-shaped	257	262	16.2	0.840
γ-Al_2O_3–$NaAlO_2$/PCC	PCC	Cylindrical	198	247	8.9	0.530

S_{BET}–surface area by method Brunauer–Emmett–Teller (BET), m^2/g [17]

S_{mesop}–surface area by method Barrett–Joyner–Halenda (BJH), m^2/g [17, 18]

D_p–pore diameter, nm

V_p–pore volume, cm^3/g

coincides with the classical type (type H3) and corresponds to the presence of slit-shaped pores, which agrees well with the small-angle X-ray diffraction data [20]. However, the pore size distribution of the sample (γ-Al_2O_3/PCC) is quite characteristic of layered materials, with a narrow maximum in the region of 3–13 nm (Table 2).

Previously, it was shown that the introduction of sodium aluminate into γ-Al_2O_3 system led to the formation of cylindrical pores Type H1 [5]. However, the surface area of the samples, consisting of sodium aluminate (γ-Al_2O_3–$NaAlO_2$/PEI), decreased with increasing of the pore size. These changes confirm the changing of the internal structure of the samples. Of particular interest are the γ-Al_2O_3–$NaAlO_2$ samples obtained using Pluronic P123 and PCC as the templates. In the case of introducing an individual template, P123 and PCC, into the γ-Al_2O_3–$NaAlO_2$ system, not only the pore size but also their shape changed. In particular, the hysteresis profile of the γ-Al_2O_3–$NaAlO_2$/P123 coincides with the classical type (Type H3) and corresponds to the presence of slit-shaped pores [17]. Compared with γ-Al_2O_3/P123 sample obtained without application of sodium aluminate as the additive, the BET surface area of the γ-Al_2O_3–$NaAlO_2$/P123 sample decreases insignificantly to 257 m^2/g, whereas the pore diameter doubled increases to 16.2 nm, which is typical of ordered mesoporous materials (Table 2). The γ-Al_2O_3–$NaAlO_2$/PCC sample obtained using PCC also has a hysteresis loop in the mesopore region (Fig. 3e). In this case, the hysteresis loop shape of this sample coincides with the classical one (Type H1) and corresponds to the presence of cylindrical pores. Compared to the γ-Al_2O_3/PCC sample, the BET surface area of γ-Al_2O_3–$NaAlO_2$/PCC significantly decreases from 297 m^2/g to 198 m^2/g, whereas the pore diameter slightly decreases from 105 nm to 8.9 nm, which is typical of ordered mesoporous materials (Fig. 3f).

3.4 Microscopic studies, SEM, AFM, and TEM

The results of SEM of the non-annealed and annealed γ-Al_2O_3 samples obtained with application of such templates as PEI, P123, PCC, are presented in Fig. 4a–c. The formation of porous materials during the synthesis process can be observed via SEM images.

As a result of the calcination of the γ-Al_2O_3/template samples at 600 °C, the burnout of organic templates and formation of a more highly developed structure with increased surface area values and a narrower pore size distribution compared to γ-Al_2O_3 has occurred (Table 2). These results are in a good agreement with the XRD results of the Al_2O_3–$NaAlO_2$/template samples showing the presence of the boehmite phase before samples calcination and γ-alumina phase after calcination of the samples at 600 °C.

The results of SEM and EDX analysis of the non-annealed and annealed γ-Al_2O_3–$NaAlO_2$ samples obtained with application of such templates as PEI, P123, PCC, are presented in Figs 5 and 6. The SEM images showed that the γ-Al_2O_3–$NaAlO_2$/PEI and γ-Al_2O_3–$NaAlO_2$/P123 samples have a well-formed structure, whereas the Al_2O_3–$NaAlO_2$/PCC sample has a partially amorphous structure.

The SEM–EDX (energy-dispersive X-ray) analysis showed that the surface composition of γ-Al_2O_3–$NaAlO_2$/template obtained using different templates has different sodium content in the surface layer that has a direct effect on the catalytic properties of these materials. The EDS analysis showed the sodium content in the γ-Al_2O_3–$NaAlO_2$/PEI, Al_2O_3–$NaAlO_2$/P123, and Al_2O_3–$NaAlO_2$/PCC samples was found to be ~0.25%, 3.80%, and 0.47%, respectively (Fig. 5a–c). These obtained results are in a good agreement with the XRD results of the Al_2O_3–$NaAlO_2$/template samples showing the presence of γ-alumina and sodium aluminate phases in the samples both before and

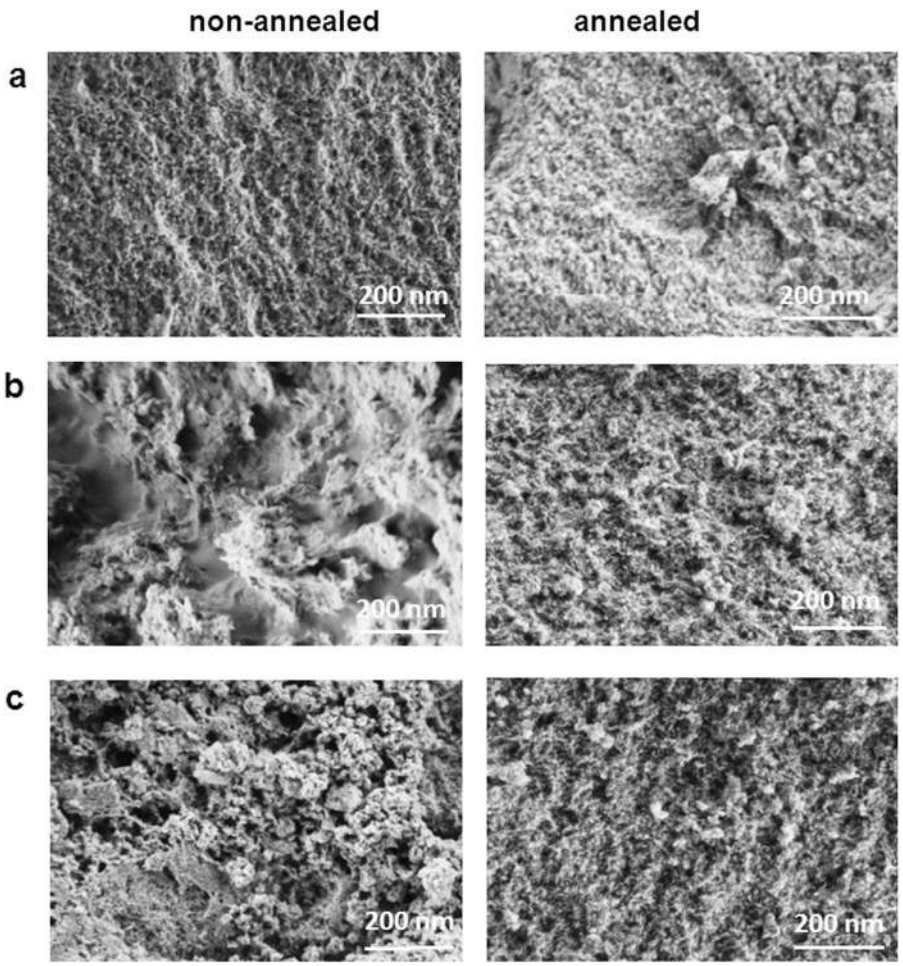

Fig. 4 Results of SEM of the γ-Al_2O_3 sample obtained with templates: **a** PEI; **b** P123; **c** PCC

after calcination (Fig. 2a–c). Dissolution of the sodium aluminate phase in alumina occurs at temperature exposure. At the same time, for different types of templates, both individual and as in the form of PCCs, this effect is preserved. It should be noted that as a result of heat treatment, the main part of the sodium aluminate phase is in the bulk of the material, whereas only its insignificant part is on the surface (Fig. 5). These data are in good agreement with the results obtained by us earlier [5], showing the formation of the mesoporous structure in the Al_2O_3–$NaAlO_2$ system with the usage of PEI as the template. This may be owing to the sodium aluminate interaction with the melt of the template at high temperature, namely its dissolution in the melt.

After calcination of all samples at 600 °C, the organic phase is removed and an ordered mesoporous structure is formed. All γ-Al_2O_3–$NaAlO_2$/template composites after calcination have a structure with high surface area values compared with Al_2O_3–$NaAlO_2$ obtained without heat treatment (Table 2). The grainy structure of the calcined γ-Al_2O_3–$NaAlO_2$/PCC responsible for the observed relatively larger mesopores is clearly distinguishable in the AFM image (Fig. 6d), contrasting to the smaller mesopores in the more amorphous as-synthesized material showing more smooth surface. The nucleation of the solid metal oxide phase in the form of distinct nanoparticles is a general feature in the sol-gel process, reflecting the so-called Micelle Templated by Self-Assembly of Ligands (MTSAL) mechanism. The particles resemble the Poly-Oxo-Metallate ions with dense oxide cores and amorphous shell containing residual organic and hydroxide ligands [21]. The particles are also clearly distinguishable in the TEM images, where they are assembles in the nanostructures pre-designed by aggregation driven by utilized polymer surfactants (see Figs 7 and 8).

3.5 Supramolecular self-assembly of nanostructures

Amphiphilic molecules can be assembled in micellar aqueous solutions into different structures. The most-probable shape and size of the ensemble are determined by the particle structure and packing that depends on a number of external factors (temperature, solvent, medium pH, etc.). The nature of the bonds between PEI, P123, and aluminum hydroxide sol particles determines the self-assembly

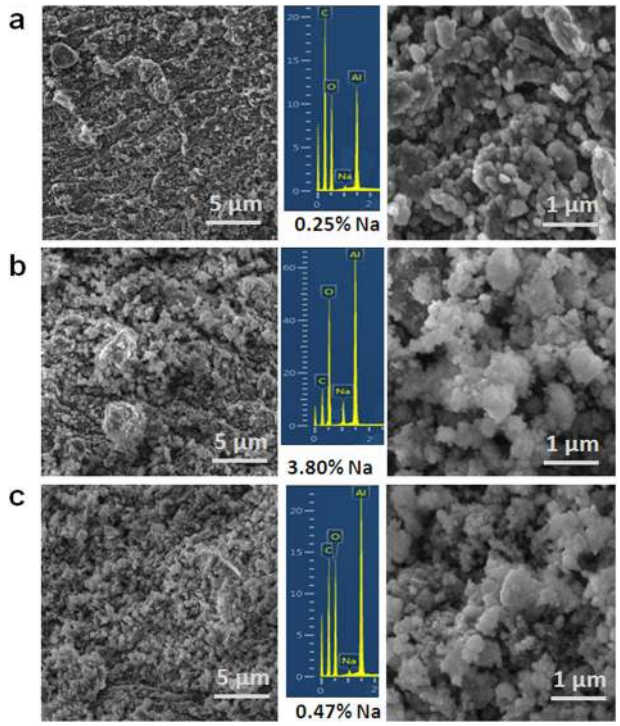

Fig. 5 Results of SEM and EDX analysis of the γ-Al_2O_3–$NaAlO_2$ sample obtained with templates: PEI **a**; P123 **b**; PCC **c**

mechanism of PCCs. Based on the obtained results of hysteresis loop profiles and the ordered pore size distribution of the synthesized samples, it is possible to suppose how templates interact with the boehmite sol particles. The scheme of the possible formation of aluminum oxide nanostructures by using the templates (PEI, P123, and PCC) is presented in Fig. 7.

Complexation is probably caused by the electrostatic interaction of PEI and sol particles. As a result, the sol molecules form a packing on the polyelectrolyte surface with formation of rod-like structures aggregated further in hedgehog like blocks (Fig. 7a). Using P123 as the template also leads to the formation of packaging. The added sol particles interact with the surfactant and cover the formed micellar framework even in this case with dominating rod-like shape (Fig. 7b). The annealing of both systems results in organic phase removal and formation of the final mesostructured framework with cylindrical pores (type H1) uniformly distributed in the sample volume [22]. The obtained materials had large surface areas and a high degree of ordering (Table 2).

If a PCC is used as the template, the mesoporous structure of aluminum oxide is formed in a different way. Having analyzed the obtained results of the low-temperature nitrogen adsorption/desorption, X-ray diffraction analysis of the final product—mesoporous aluminum oxide—it is possible to suppose that as a result of polyethylenimine interaction with Pluronic123 in aqueous solution, the surfactant molecules form a micellar structure. The polyelectrolyte interacting with P123 forms the upper layer through intermolecular interaction. The sol particles added later form the final structure of the material that features distinctly planar densified nanostructures (Fig. 7b). During drying and annealing, the organic phase is removed, which produces slit-shaped pores (type H3) [22] that can be distinguished in the TEM images (Fig. 7c). By using PCC, we have managed to enlarge the pores to 10 nm in size, compared with the synthesis results in the presence of individual templates, but preserved the large surface area—297 m^2/g_{BET}—and changed the shape of the mesoporous material pores from the cylindrical to slit-like one.

Based on the obtained results of hysteresis loop profiles and SEM of the samples, it is possible to suppose the mechanism of the interaction of the boehmite sol particles with sodium aluminate structures (Fig. 8a–c).

The formation of the mesoporous structures of the γ-Al_2O_3–$NaAlO_2$ sample with the usage of PEI occurs in a similar way to the above-described scheme (Fig. 7a). Perhaps, the introduction of sodium aluminate at the final stage of the synthesis has contributed to the formation of much larger pores, but smaller surface area than in case of the γ-Al_2O_3 sample synthesized by using PEI as the template (Fig. 7a). During annealing of the samples, the organic phase is removed, which produces a mesostructured framework with cylindrical pores (Fig. 8a) as it is also visible in the TEM image.

However, the self-assembly process of the mesoporous structure of aluminum oxide using Pluronic P123 and the PCC with the addition of sodium aluminate occurs in a different way. Based on the results obtained from the low-temperature N_2 adsorption–desorption experiments, it is possible to suppose that the introduction of individual synthesis template together with sodium aluminate contributes to the formation of planar structure micelles in aqueous solution (Fig. 8b). Then, the added sol particles interact with the surfactant and cover the already formed micellar framework. The particles of sodium aluminate introduced at the final stage of the synthesis are distributed in the volume of the formed structure. During drying and annealing, the organic phase is removed, which produces slit-shaped pores (type H3) [22]. Thus, the BET surface area and pore diameter of (γ-Al_2O_3–$NaAlO_2$/P123) was 119 m^2/g and 11.6 nm, respectively. The planar structures in this case are noticeably thicker, confirming possible enlargement of the original alumina structure in planar micelles by additional growth owing to charge interactions with negatively charged basic sodium aluminate nanoparticles.

Based on the low-temperature N_2 adsorption–desorption results, it can also be proposed that when PEI reacts with Pluronic P123 in the aqueous solution, surfactant molecules form a package (Fig. 8c). Polyelectrolyte by interacting with

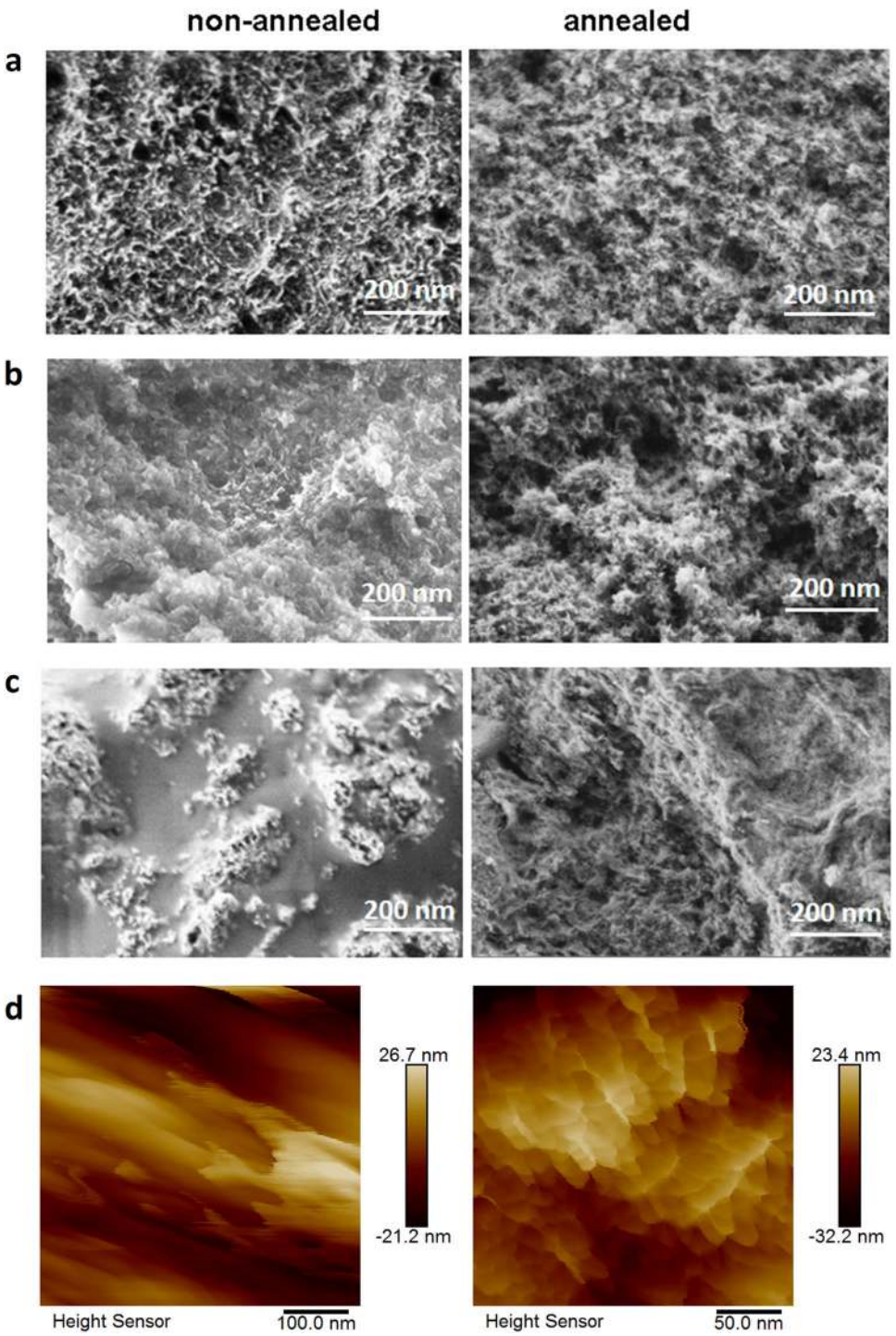

Fig. 6 Results of SEM studies of the γ-Al_2O_3–$NaAlO_2$ sample obtained with templates: PEI **a**; P123 **b**; PCC **c**; and of AFM study of the PCC-derived sample **d**

Pluronic P123 forms the upper layer owing to intermolecular interaction. Then, the added sol particles form the final structure of the material, whereas sodium aluminate particles are distributed in the structure obtained earlier. During drying and annealing, the organic phase is removed, which produces a mesostructured framework with cylindrical pores (type H1). Thus, the γ-Al_2O_3–$NaAlO_2$/PCC sample with BET surface area and pore diameter of 198 m^2/g and 9 nm were obtained, respectively. Here, both rod-like and densified planar structure fragments can be clearly seen.

4 Conclusions

We have successfully investigated the influence of $NaAlO_2$ on the formation of the internal mesoporous structure of

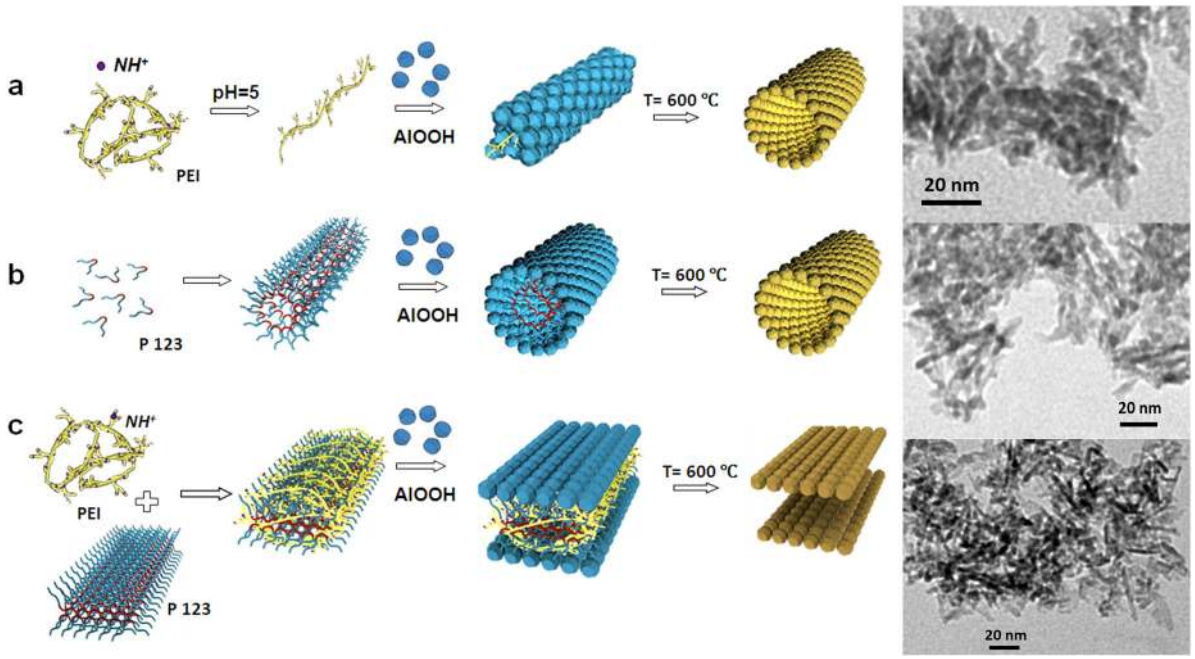

Fig. 7 Possible formation mechanism of nanostructures of aluminum oxide using templates: PEI **a**; P123 **b**; PCC **c**

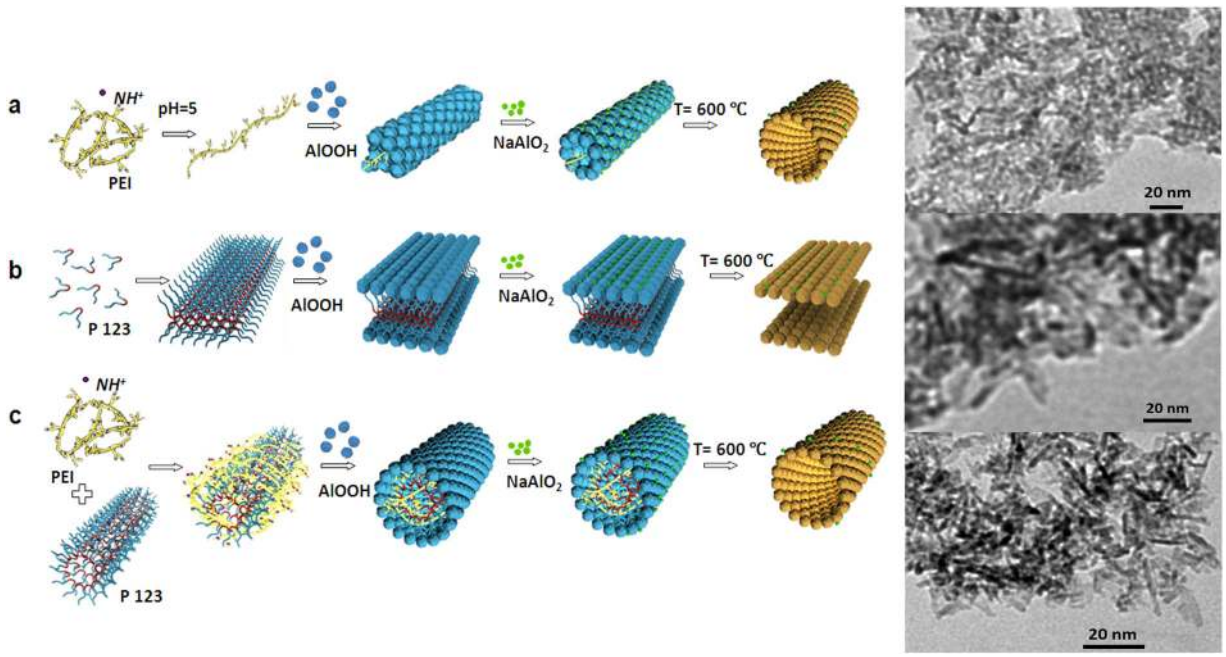

Fig. 8 Possible formation mechanism of nanostructures of γ-Al_2O_3–$NaAlO_2$ using templates: PEI **a**; P123 **b**; PCC **c**

aluminum oxide obtained by sol–gel synthesis in the presence of the individual templates (polyethylenimine and Pluronic123) and the PCC formed by the interaction of individual surfactants in the solution. Depending on the application of different templates and their polymer–colloid complexes, with and without the addition of $NaAlO_2$, the mesostructured γ-aluminum oxide with different morphology, pore size, and specific surface area was obtained. It was shown that mesostructured aluminum oxide obtained using individual templates possess cylindrical pores, whereas applying PCC resulted in the formation slit-shaped pores. Introduction of sodium aluminate to the synthesis of γ-Al_2O_3 allows to vary both pore size and shape of Al_2O_3. Production of mesoporous

γ-Al_2O_3–$NaAlO_2$ composite with the application of PEI and PCC allows to form cylindrical pores while applying individual surfactants resulted in the formation slit-shaped pores. The proposed mechanisms were visualized by high-resolution AFM and TEM studies that clearly confirmed the proposed transformation pathways. Thus, by applying "soft chemistry" with the usage of different templates and their PCCs, it is possible to vary the size of the obtained porous materials, their structure, and therefore to adapt the synthesized materials for a specific chemical process.

Acknowledgements The research was carried out within the framework of the State Program "Scientific and technological foundations of the production of functional materials and nanocomposites" (No. 0092-2018-0003) and supported by RFBR, according to the research project No. 18-33-00808. We are grateful to Dr. O.L. Evdokimova for helpful discussions and suggestions.

Compliance with ethical standards

Conflict of interest The authors declare that they have no conflict of interest.

References

1. Liu X, Wei Y, Jin W, Shih W-H (2000) Synthesis of mesoporous aluminum oxide with aluminum alkoxide and tartaric acid. Mater Lett 42:143–149
2. Misra C (1986) Industrial alumina chemicals. ACS Monograph, Washington
3. Hochepied J-F, Nortier P (2002) Influence of precipitation conditions (Ph and temperature) on the morphology and porosity of boehmite particles. Powder Tech 128:268–272
4. Rambidi NG, Berezkin AV (2009) Physical and chemical bases of nanotechnologies. Fizmalit, Moscow
5. Agafonov AV, Yamanovskaya IA, Ivanov VK et al. (2015) Controlling micro- and nanostructure and activity of the $NaAlO_2$ biodiesel transesterification catalyst by its dissolution in a mesoporous γ-Al_2O_3-matrix. J Solgel Sci Technol 76:90–97
6. Vinogradov VV, Agafonov AV, Vinogradov AV et al. (2011) Synthesis of organized mesoporous γ-alumina templated with polymer–colloidal complex. J Solgel Sci Technol 60:6–10
7. Yamanovskayaa IA, Gerasimova TV, Agafonov AV (2018) Using polymer-colloid complexes for obtaining mesoporous aluminium oxide by the template sol-gel method. Russ J Inorg Chem https://doi.org/10.1134/S0044457X18090210
8. Ren B, Fan M, Tan L et al. (2016) Electrospinning synthesis of porous Al_2O_3 nanofibers by pluronic P123 triblock copolymer surfactant and properties of uranium (VI)-sorption Mater Chem Phys 177:190–197
9. Brinker CJ, Scherer GW (1990) Sol-gel science: the physics and chemistry of sol-gel processing. Academic Press, San Diego
10. Niesz K, Yang P, Somorjai GA (2005) Sol-gel synthesis of ordered mesoporous alumina. Chem Commun 0:1986–1987
11. Monnier A, Schuth F, Huo Q et al. (1993) Cooperative formation of inorganic-organic interfaces in the synthesis of silicate mesostructures. Science 261:1299–1303
12. Deng W, Bodart P, Pruski M, Shanks BH (2002) Characterization of mesoporous alumina molecular sieves synthesized by nonionic templating. Microporous Mesoporous Mater 52:169–177
13. Holmberg K., Jönsson B., Kronberg B., Lindman B. (2007) Surface-active substances and polymers in solutions. Binom, Moscow
14. Spivak YM (2013) Nanostructured materials. Features of reception and diagnostics. Izvestiya of higher educational institutions of Russia. Radio-Electronics 6:54–64
15. Len J-M (1998) Supramolecular chemistry. Concepts and prospects. Nauka, Novosibirsk
16. Yoldas BE (1975) A transparent porous alumina. Am Ceram Soc Bull 54:286–288
17. Rouquerol J, Rouquerol F, Llewellyn P, Maurin G, Sing K (1998) Adsorption by powders and porous solids. Elsevier, Amsterdam
18. Brunauer S (1938) Adsorption of gases in multimolecular layers. J Amer Chem Soc 60:309–319
19. Nakamoto K (1965) Infrared spectra and the structure of organic compounds. Mir, Moscow
20. Ariga K, Hill JP, Ji Q (2007) Layer-by-layer assembly as a versatile bottom-up nanofabrication technique for exploratory research and realistic application. Phys Chem Chem Phys 9:2319–2340
21. Seisenbaeva GA, Kessler VG (2014) Precursor directed synthesis – "molecular" mechanisms in the Soft Chemistry approaches and their use for template-free synthesis of metal, metal oxide and metal chalcogenide nanoparticles and nanostructures. Nanoscale 6:6229–6244
22. Novakov IA, Radchenko FS, Pastukhov AS, Papisov IM (2005) Investigation of the properties of aqueous solutions of polymer-colloidal complexes of polyacrylamide and aluminum polyhydroxochloride. High Highlight Cpd 47:73–77